



# Inhomogeneous nuclear spin flips: Feedback mechanism between electronic states in a double quantum dot and the underlying nuclear spin bath

The Harvard community has made this  
article openly available. [Please share](#) how  
this access benefits you. Your story matters

Citation	Stopa, M., J. J. Krich, and A. Yacoby. 2010. "Inhomogeneous Nuclear Spin Flips: Feedback Mechanism between Electronic States in a Double Quantum Dot and the Underlying Nuclear Spin Bath." <i>Physical Review B</i> 81 (4). <a href="https://doi.org/10.1103/physrevb.81.041304">https://doi.org/10.1103/physrevb.81.041304</a> .
Citable link	<a href="http://nrs.harvard.edu/urn-3:HUL.InstRepos:41412147">http://nrs.harvard.edu/urn-3:HUL.InstRepos:41412147</a>
Terms of Use	This article was downloaded from Harvard University's DASH repository, and is made available under the terms and conditions applicable to Open Access Policy Articles, as set forth at <a href="http://nrs.harvard.edu/urn-3:HUL.InstRepos:dash.current.terms-of-use#OAP">http://nrs.harvard.edu/urn-3:HUL.InstRepos:dash.current.terms-of-use#OAP</a>

# Inhomogeneous Nuclear Spin Flips

M. Stopa,<sup>1,\*</sup> J. J. Krich,<sup>2</sup> and A. Yacoby<sup>2</sup>

<sup>1</sup>Center for Nanoscale Systems, Harvard University, Cambridge, MA 02138

<sup>2</sup>Department of Physics, Harvard University, Cambridge, MA 02138

We discuss a feedback mechanism between electronic states in a double quantum dot and the underlying nuclear spin bath. We analyze two pumping cycles for which this feedback provides a force for the Overhauser fields of the two dots to either equilibrate or diverge. Which of these effects is favored depends on the g-factor and Overhauser coupling constant  $A$  of the material. The strength of the effect increases with  $A/V_x$ , where  $V_x$  is the exchange matrix element, and also increases as the external magnetic field  $B_{ext}$  decreases.

PACS numbers: 03.67.Lx, 73.21.La, 71.15.-m

Hyperfine interaction with the host nuclei in nanoscale GaAs systems, while relatively weak, can nevertheless limit the electron coherence time and thereby complicate strategies to implement quantum information and quantum computing schemes in these systems [1, 2, 3, 4]. Conversely, ever-increasing control of angular momentum transfer between electrons and nuclei in a range of materials enables numerous applications precisely because of the environmental isolation of the nuclear system. These include applications to quantum information processing employing NMR [5]. From the perspective of fundamental physics, experiments on few-electron systems with controllable coupling to the nuclear many-body system uncover a fascinating arena of new phenomena with ramifications for theoretical physics and engineering [6].

Experiments on double quantum dots with electron number  $N = 2$  have uncovered and exploited an intriguing phenomenon called the “Pauli blockade” [7] in which two electrons with parallel spins are forbidden from combining in one dot by the exclusion principal. In transport or in gate pulsing, even when such a transition becomes energetically favorable, it can only proceed via a spin “flip-flop” process in which angular momentum is exchanged with the local nuclei. Repeating the spin transfer modifies the character of the nuclear spin distribution. One metric for the nuclear state is the difference between the total Overhauser fields of each dot. These are the effective Zeeman fields which the electrons experience due to nuclear polarization. Several recent experiments addressed transfer of angular momentum from the electron system to the nuclear bath through various pumping cycles. One experiment claims that under a specific, repeated pulsing sequence (see below) [8] the polarizations in the two dots tend to equilibrate; a phenomenon which has been numerically reproduced [9, 10]. However, another similar experiment claims to find a large difference induced between the Overhauser fields of the two dots [11]. The theory which we describe here does not claim to explain either experiment.

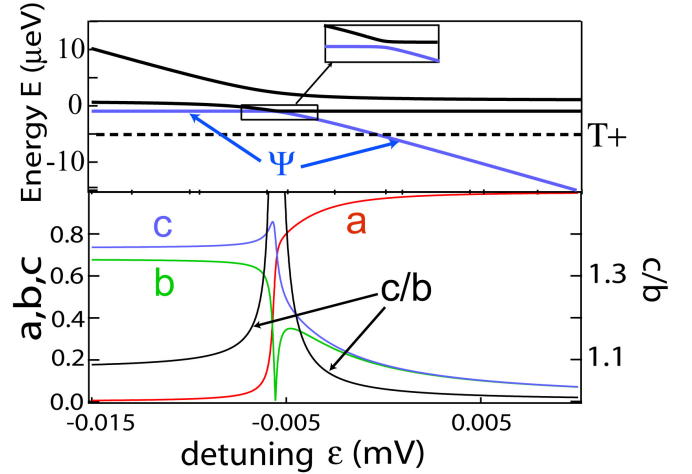


FIG. 1: Top: electronic states near the (1,1) to (0,2) stability diagram transition. Bottom: overlap of the  $\Psi$  state with  $S(0,2)$  (a), with  $|L\uparrow R\downarrow\rangle$  (b) and with  $|L\downarrow R\uparrow\rangle$  (c). Parameters:  $B_{ext} = 0.2T$ ,  $\gamma = 1.2 \mu\text{eV}$ ,  $\Delta = 1000$ ,  $E_C = 0.6\text{meV}$ ,  $V_x = 1\mu\text{eV}$ .

Here we describe a force toward either equalizing or inducing differences between the Overhauser fields in the two dots. The direction of this force depends on the spin of the initial electron state (i.e. the direction of the electron-nuclear “flip-flop” process) as well as on the sign of the product of the g-factor  $g$  of the host material and the sign of the Overhauser magnetic field of the nuclei of Ga and As as compared to the direction of the nuclear spin (they are anti-parallel). Assuming GaAs, we describe two pulse sequences which differ in the choice of the initial electron state, which consequently have a force tending to cause the Overhauser fields in the two dots to equilibrate or to diverge.

*Electronic States of the Double Dot with  $N=2$*  - We calculate the electronic states of the two electron ( $N = 2$ ) double dot within the Hund-Mulliken formalism [12] de-

\*Electronic address: stopa@cns.fas.harvard.edu

veloped for the hydrogen molecule. Typically, in this method, eigenstates of total spin, singlets and triplets, are employed as basis states. However, since we wish to study the inhomogeneous Overhauser effect due to different effective magnetic fields in the two dots, we choose a basis which diagonalizes, at the single particle level, the z-component of this inhomogeneous field and in which the spatial dependence of nuclear spin flips induced by electronic spin ‘‘flops’’ is transparent. The basis is:  $\{\xi_n\} \equiv \{|R_\uparrow R_\downarrow\rangle, |L_\uparrow R_\downarrow\rangle, |L_\downarrow R_\uparrow\rangle, |L_\uparrow R_\uparrow\rangle\}$ , where L and R indicate the orbital states of the left and right dot, the arrows denote spin direction [13]. Two remaining states of the Hund-Mulliken model,  $|L_\downarrow R_\downarrow\rangle$  and  $|L_\uparrow L_\uparrow\rangle$  are not relevant to our analysis. Note that  $|R_\uparrow R_\downarrow\rangle$  is the standard  $S(0, 2)$  state and  $|L_\uparrow R_\uparrow\rangle$  is the standard  $|T^+\rangle$  state. The hyperfine Hamiltonian for two electrons is properly

written:

$$H_{hf} = \frac{vA}{\hbar^2} \sum_m^M [\delta(\mathbf{r}_1 - \mathbf{R}_m) \mathbf{S}_1 \cdot \mathbf{I}_m \otimes \mathbf{1} + \mathbf{1} \otimes \delta(\mathbf{r}_2 - \mathbf{R}_m) \mathbf{S}_2 \cdot \mathbf{I}_m] \quad (1)$$

where  $\mathbf{r}_i$  and  $\mathbf{S}_i$  are operators in the subspace of electron  $i$  (first quantized representation) and  $m$  is summed over a total of  $M$  nuclei (typically  $M \sim 10^6$ ); and where  $v$  is the volume per nucleus. We assume, for simplicity, a single nuclear species with spin  $1/2$ . Then, constraining the maximum Overhauser field to be  $5.3T$  [14] leads to a coupling constant  $A = -270 \mu eV$ . We incorporate the matrix elements of  $H_{hf}$  from Eq. 1 in our basis  $\{\xi_n\}$  into the Hund-Mulliken Hamiltonian which gives

$$H = \begin{pmatrix} |R_\uparrow R_\downarrow\rangle & |L_\uparrow R_\downarrow\rangle & |L_\downarrow R_\uparrow\rangle & |L_\uparrow R_\uparrow\rangle \\ \left( E_C - \varepsilon \right. & I_z^{LR} - I_z^{RR} \langle L|R \rangle + \gamma & I_z^{LR} - I_z^{RR} \langle L|R \rangle + \gamma & I_+^{RR} \langle L|R \rangle - I_+^{LR} \\ & I_z^{LL} - I_z^{RR} & V_x & I_+^{RR} \\ & & I_z^{RR} - I_z^{LL} & I_+^{LL} \\ & & & I_z^{RR} + I_z^{LL} + E_Z \end{pmatrix}, \quad (2)$$

which is correct to leading order in  $\langle L|R \rangle$ , where  $\varepsilon$  is the potential ‘‘detuning’’ (the difference between the electrostatic potential bottom of the left and right dots) and where we have taken the orbital energies of  $L$  and  $R$  to be zero for simplicity. We include only two Coulomb terms: the charging energy  $E_C \equiv V_{RRRR} - V_{RLRL}$  and the exchange matrix element  $V_x \equiv V_{LRRL}$  [15]. Also in Eq. 2,  $\gamma$  is the tunneling coefficient;  $E_Z \equiv g\mu_B B_{ext}$  is the Zeeman energy for a presumed external field  $B_{ext}$ , which defines the z-axis of the problem, with  $\mu_B$  the Bohr magneton. The lower left hand side of the matrix is the complex conjugate of the upper right hand side. Note that the matrix elements of  $H$  in this electronic basis remain operators in the Hilbert space of the nuclear coordinates [16]:

$$\vec{I}^{\alpha\beta} \equiv v \frac{A}{2\hbar} \sum_{m=1}^M \psi_\alpha^*(\mathbf{R}_m) \psi_\beta(\mathbf{R}_m) \vec{I}_m \quad (3)$$

where  $\alpha, \beta \in \{L, R\}$ . Note that previous researchers have typically ignored the transition term  $I_+^{LR}$ , which we see from Eq. 2 can lead to a direct transition between  $|R_\uparrow R_\downarrow\rangle$  and  $|L_\uparrow R_\uparrow\rangle$  and causes a spin flip *in the barrier*. This term, and the other overlap terms (e.g.  $\propto \langle L|R \rangle$ ), could be significant in the case of large  $B_{ext}$  and small  $\gamma$ , i.e. where  $|R_\uparrow R_\downarrow\rangle$  and  $|L_\uparrow R_\uparrow\rangle$  anti-cross deep in the (0,2) regime. However we will henceforth ignore hyperfine terms in Eq. 2 proportional to wavefunction overlap (e.g.  $\langle L|R \rangle$  and  $I_+^{LR}$ ) and leave exploration of the barrier nuclear spin flip to a later publication [17].

*Nuclear spin flip location* - The crucial feature of Eq.

2 is that the  $|L_\uparrow R_\uparrow\rangle$  state is coupled to  $|L_\uparrow R_\downarrow\rangle$  via a term which flips a nuclear spin in the right dot ( $I_+^{RR}$ ) and it is coupled to  $|L_\downarrow R_\uparrow\rangle$  by a term that flips a nuclear spin in the left dot ( $I_+^{LL}$ ). In the *absence* of flip-flop coupling to the  $|L_\uparrow R_\uparrow\rangle$  state, the upper left 3x3 matrix in Eq. 2 (see also yellow highlighted region of Fig. 2) has a ground state, which we denote:

$$|\Psi\rangle = a(\varepsilon) |R_\uparrow R_\downarrow\rangle + b(\varepsilon) |L_\uparrow R_\downarrow\rangle + c(\varepsilon) |L_\downarrow R_\uparrow\rangle. \quad (4)$$

As shown in figure 1, at large (positive)  $\varepsilon$ ,  $|\Psi\rangle \rightarrow |R_\uparrow R_\downarrow\rangle \equiv S(0, 2)$  and at large negative  $\varepsilon$ ,  $|\Psi\rangle$  becomes an unequal superposition of  $|L_\uparrow R_\downarrow\rangle$  and  $|L_\downarrow R_\uparrow\rangle$ . Even when  $V_x > |\langle I_z^{RR} - I_z^{LL} \rangle|$ , the inhomogeneous Overhauser effect will produce a preference for either the  $|L_\uparrow R_\downarrow\rangle$  or the  $|L_\downarrow R_\uparrow\rangle$  component of  $\Psi$  (see figure 1), with the electron down spin preferentially located on the dot with smaller  $I_z$ . In the first electron pulsing sequence which we describe, the electron state is initialized at large  $\varepsilon$  into  $|\Psi\rangle \approx S(0, 2)$  and detuning is swept approximately adiabatically through the  $\Psi - |L_\uparrow R_\uparrow\rangle$  anti-crossing. The position of this anti-crossing,  $\tilde{\varepsilon}$ , is determined by the energy of  $|L_\uparrow R_\uparrow\rangle \equiv |T^+\rangle$ , denoted  $E(T^+)$  (see figure 1), which is determined by  $B_{ext}$ . Insofar as  $b(\tilde{\varepsilon}) \neq c(\tilde{\varepsilon})$ , a transition from  $\Psi$  to  $|L_\uparrow R_\uparrow\rangle$  will preferentially induce a nuclear spin flip (down) on the side with the larger  $I_z$ . This tends to equilibrate the values of  $I_z^{RR}$  and  $I_z^{LL}$ . In the second pulse sequence the electrons are initialized into  $|L_\uparrow R_\uparrow\rangle$  and the state then transitions to  $\Psi$ . The same feedback mechanism preferentially now causes nuclear spins to flip *up*, but still on the side with the larger  $I_z$ , thus leading

to a tendency for  $|I_z^{LL} - I_z^{RR}|$  to grow. Both of these sequences can be experimentally implemented [11, 18]. Our further analysis focuses mainly on the first pulse sequence.

Note that the preceding argument depends on the *sign* of  $A$  which in turn depends on the sign of  $g$  and the sign of the effective Overhauser field which, for Ga and As, are anti-parallel to the nuclear spins [19].

*Nuclear States* -To further analyze the Hamiltonian, Eq. 2, it is helpful to introduce a simplified basis for the nuclear states in which all of the nuclei are either in the left or right dot and all within a given dot interact equally with the electron. In other words,  $|\psi_L(\mathbf{r})|^2$  is taken as a constant within a spherical “box” of some volume,  $\mathcal{V}$ . In this model, which we refer to as the “box model,” the squares of the total angular momenta  $I_\alpha^2$  are conserved, where  $\vec{I}_\alpha \equiv (vA/\mathcal{V}) \sum_{m \in \alpha} \vec{I}_m$ , and where  $\alpha \in \{L, R\}$ . Thus, the electrons essentially interact with two composite nuclear spins, one on the left and one on the right. The nuclear state basis is  $\{I_L, I_R, I_{Lz}, I_{Rz}\}$  (where  $I_\alpha(I_\alpha + 1)$  is the eigenvalue of  $(\vec{I}^{\alpha\alpha})^2$  and  $I_{\alpha z}$  is the eigenvalue of  $I_z^{\alpha\alpha}$ ). Finally, for given  $I_L, I_R$ , it is convenient to transform to the basis of  $\Delta \equiv I_{Lz} - I_{Rz}$  and  $s \equiv I_{Lz} + I_{Rz}$ . In this basis the z-components of the nuclear operators have non-zero matrix elements on the diagonal blocks, but the raising and lowering operators connect different  $(\Delta, s)$  subspaces (see Fig. 2).

The strength of the narrowing force depends on the ratio  $r \equiv c/b$  at  $\tilde{\varepsilon}$ . This depends on  $\Delta$  and on  $B_{ext}$ . For example, smaller  $B_{ext}$  results in smaller (or more negative)  $\tilde{\varepsilon}$ , where, as shown in Fig. 1, the ratio  $c/b$  increases (for  $\Delta > 0$ ). Exactly *how* large  $c/b$  can get depends on  $V_x$  which, in the example of Fig. 1, we have set to  $1 \mu\text{eV}$  [20].

In Fig. 3 we plot the value of  $r(\tilde{\varepsilon})$  as a function of  $B_{ext}$  for various values of  $\Delta$ . The key point is that  $r(\tilde{\varepsilon})$  increases monotonically with  $\Delta$  (cf. yellow highlighted region of Fig. 2), however it also decreases monotonically with  $B_{ext}$  (and hence  $\tilde{\varepsilon}$ ). Interestingly, because the  $|R_\uparrow R_\downarrow\rangle$  state is coupled equally to  $|L_\uparrow R_\downarrow\rangle$  and  $|L_\downarrow R_\uparrow\rangle$ , the value of  $b/c$  is *independent* of  $\gamma$ .

We note that the flip-flop process naturally also depends on the rate at which  $\varepsilon$  is swept since, in order to be adiabatic and remain on the lower branch of the  $\Psi - |L_\uparrow R_\uparrow\rangle$  anti-crossing the  $\varepsilon$  variation must be sufficiently slow. More generally, the character of the state evolution can be examined as a Landau-Zener tunneling problem [21] or else evaluated numerically [17].

The evolution of the full nuclear state is complex and the experimental manifestations of that evolution are ambiguous. Nevertheless, as a possible baseline for more detailed studies of the nuclear evolution, we describe a simple, incoherent model which results in narrowing of the distribution of  $\Delta$ .

If we assume that the system is in the well-defined state  $|\Psi\rangle \otimes \{I_L, I_R, I_{Lz}, I_{Rz}\}$  and the detuning is moved quickly to  $\tilde{\varepsilon}$  and held there for time  $\tau$ , we can compute, by Fermi’s golden rule, the probability for a nuclear spin

$\Delta-1, s-1$				$\Delta, s$				$\Delta+1, s-1$			
$E_{C-\varepsilon}$	$\gamma$	$\gamma$	0	0	0	0	0	0	0	0	0
$\gamma^*$	$\Delta-1$	$V_x$	0	0	0	0	0	0	0	0	0
$\gamma^*$	$V_x^*$	$-\Delta-1$	0	0	0	0	0	0	0	0	0
0	0	0	$s-1+E_z$	0	$I_R$	0	0	0	0	0	0
0	0	0	0	$E_{C-\varepsilon}$	$\gamma$	$\gamma$	0	0	0	0	0
0	0	0	$I_{R+}$	$\gamma^*$	$\Delta$	$V_x$	0	0	0	0	0
0	0	0	0	$\gamma^*$	$V_x^*$	$-\Delta$	0	0	0	0	$I_{L+}$
0	0	0	0	0	0	0	$s+E_z$	0	0	0	0
0	0	0	0	0	0	0	0	$E_{C-\varepsilon}$	$\gamma$	$\gamma$	0
0	0	0	0	0	0	0	0	$\gamma^*$	$\Delta+1$	$V_x$	0
0	0	0	0	0	0	0	0	$\gamma^*$	$V_x^*$	$-\Delta+1$	0
0	0	0	0	0	0	$I_L$	0	0	0	0	$s+1+E_z$

FIG. 2: Hamiltonian for three sectors of the nuclear difference quantum number  $(\Delta - 1, s - 1)$ ,  $(\Delta, s)$ ,  $(\Delta + 1, s - 1)$ . In the above,  $\pm\Delta \pm 1$  and  $s \pm 1$  are shorthand for  $(vA/\mathcal{V})(\pm\Delta \pm 1)$  and  $(vA/\mathcal{V})(s \pm 1)$  respectively.

to flip in the right dot as:

$$\begin{aligned}
\Gamma_R(I_{Lz}, I_{Rz} \rightarrow I_{Lz}, I_{Rz} - 1) &\equiv \Gamma_R(s, \Delta \rightarrow s - 1, \Delta - 1) \\
&= \frac{\tau^2}{\hbar^2} |\langle I_{Lz} I_{Rz} - 1 | I_-^{RR} | I_{Lz} I_{Rz} \rangle|^2 \\
&= \frac{A^2 \Omega_R^2 \tau^2}{4\hbar^2} |b|^2
\end{aligned} \tag{5}$$

where we have suppressed the  $I_L, I_R$  dependence for brevity and where the matrix elements of the ladder operators are given by the well-known formulas:  $\Omega_{\alpha\pm} \equiv \langle I_\alpha, I_{\alpha z} \pm 1 | I_\pm | I_\alpha, I_{\alpha z} \rangle = \sqrt{I_\alpha(I_\alpha + 1) - I_{\alpha z}(I_{\alpha z} \pm 1)}$ . Similarly, the flip probability in the left dot is proportional to the  $c$  component of  $\Psi$

$$\Gamma_L(s, \Delta \rightarrow s - 1, \Delta + 1) = \frac{A^2 \Omega_L^2 \tau^2}{4\hbar^2} |c|^2. \tag{6}$$

If we denote the probability distribution for the nuclear state (at fixed  $I_L, I_R$ ) as  $W(s, \Delta)$ , then the condition for  $W$  to be stable in its dependence on  $\Delta$  can be written (cf. Fig. 4a):

$$\begin{aligned}
W(s+1, \Delta+1) \Gamma_L(s+1, \Delta+1) &= W(s, \Delta) \Gamma_R(s, \Delta) \\
W(s, \Delta+1) &= W(s, \Delta) \frac{\Omega_{R-}^2(s, \Delta)}{\Omega_{L-}^2(s, \Delta+1)} \frac{|b(\Delta)|^2}{|c(\Delta+1)|^2}
\end{aligned} \tag{7}$$

where we have assumed that  $W(s) \approx W(s+1)$  and we have used the fact that  $b$  and  $c$  depend very weakly on  $s$  (only through the  $s$ -dependence of  $\tilde{\varepsilon}$ ).

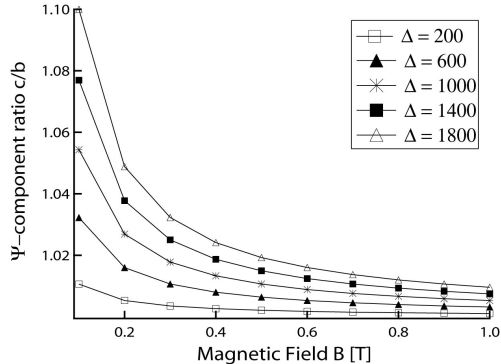


FIG. 3: The wave function ratio  $r \equiv c/b$  evaluated at the  $\Psi - T+$  crossing point,  $\tilde{\varepsilon}$ , as a function of  $B_{ext}$  for various values of the nuclear spin  $z$ -component difference  $\Delta$ .  $r(\tilde{\varepsilon})$  is monotonically increasing with  $\Delta$  and decreasing with  $B_{ext}$ .

Recursion relation Eq. 7 can be solved iteratively and the influence of the narrowing force evaluated. In Fig. 4 we have plotted  $W(\Delta)$  computed with the ratio  $\Omega_{R-}/\Omega_{L-}$  set to unity to show only the narrowing from the inhomogeneous Overhauser effect described here with the same electronic parameters as in Fig. 1, and with  $I_L = I_R = 1000$ ; including the  $\Omega$ 's induces more narrowing. For comparison we show the  $T \rightarrow \infty$  thermal distribution of  $\Delta$ , averaged over  $s$ , also for  $I_L = I_R = 1000$ . Inset (a) shows the ratio of the root-mean-square (rms)  $\Delta$  in the thermal distribution,  $\sigma_T$ , to the rms  $\Delta$  with the narrowing force at varying  $B_{ext}$ ,  $\sigma(B_{ext})$ . A substantial narrowing of  $W(\Delta)$  results from the inhomogeneous Overhauser effect.

*Discussion* - Experimentally, the  $|\Psi\rangle$  to  $|L_{\uparrow}R_{\uparrow}\rangle$  pulse sequence polarizes only about 1% of the nuclei, even when running sufficient cycles to flip all of the nuclei [18]. This saturation of the nuclear polarization is still an open problem. A recent article by Yao [22] discusses a model similar to that described herein. In that paper, no mechanism for stopping the flip-flop process is proposed when the pumping continues (as it does in experiments) beyond  $\sim 10^5$  cycles. In our model, polarization will saturate when both  $I_{Lz} = -I_L$  and  $I_{Rz} = -I_R$ , implying that  $s = -I_L - I_R$ . However, the resulting distribution of  $\Delta$  will then mirror the difference in the initial distri-

butions of  $I_L$  and  $I_R$ , and hence will show no narrowing of  $W(\Delta)$ . Thus our box model can qualitatively explain the narrowing effect or the saturation, but not both.

We believe that a full understanding of these phenomena depends on the variable coupling of the electron wave

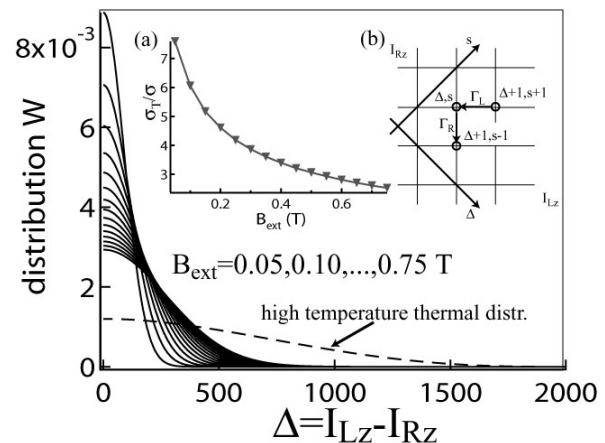


FIG. 4: (main) Reduced distribution  $W(\Delta, s)$ , calculated from Eq. 7 (solid lines), for  $V_x = 1 \mu\text{eV}$  as a function of  $\Delta$  for various  $B_{ext} = 0.05, 0.10, \dots, 0.75 \text{ T}$  (lower fields have narrower  $W$ ); and thermal  $W(\Delta)$  (dashed), averaged over  $s$ , all with  $I_L = I_R = 10^3$ . Inset (a) narrowing factor  $\sigma_T/\sigma(B_{ext})$  versus  $B_{ext}$ . Inset (b) Illustration of  $I_{Lz} - I_{Rz}$  plane.  $\Delta$  and  $s$  are the diagonal coordinates, with  $\Delta \equiv I_{Lz} - I_{Rz}$ .

function to different groups of nuclei, so that conservation of the magnitudes of two spins,  $\vec{I}_L$  and  $\vec{I}_R$ , is not required. Such a model with multiple interacting composite nuclear spins, incorporating the narrowing effect described here as well as the Landau-Zener tunneling behavior near  $\tilde{\varepsilon}$ , in some parameter regimes shows the potential to send  $|\Delta| \rightarrow 0$  while reducing the spin flip probability, slowing the growth of total polarization; for other parameters,  $|\Delta|$  grows large despite the narrowing force described here [21].

*Acknowledgments* - We thank B. I. Halperin, M. Gullans, J. Taylor, M. Lukin, S. Foletti, H. Bluhm, Y. Tokura and M. Rudner for valuable conversations. We thank the National Nanotechnology Infrastructure Network Computation Project for computational support. We gratefully acknowledge support from the Fannie and John Hertz Foundation, NSF grants PIF-0653336 and DMR-05-41988 and the ARO.

[1] A. C. Johnson *et al.*, Nature, **435**, 925 (2005).

[2] K. Ono and S. Tarucha, Phys. Rev. Lett. **92**, 256803

(2004).

[3] D. Loss and D. DiVincenzo, Phys. Rev. A **57**, 120 (1998).

- [4] W. M. Witzel and S. Das Sarma Phys. Rev. B **74**, 035322 (2006).
- [5] See, for example, L. M. K. Vandersypen and I. L. Chuang, Rev. Mod. Phys. **76**, 1037 (2004), and references therein.
- [6] R. Hanson *et al.*, Rev. Mod. Phys. **79**, 1217 (2007).
- [7] K. Ono *et al.*, Science **297**, 1313 (2002).
- [8] D. Reilly *et al.*, Science **321**, 781 (2008).
- [9] G. Ramon and X. Hu, Phys. Rev. B **75**, 161301 (2007).
- [10] H. Ribeiro and G. Burkard, arXiv:0811.3560v1
- [11] S. Foletti, H. Blum, D. Mahalu, V. Umansky and A. Yacoby, in preparation.
- [12] G. Burkard, D. Loss and D. DiVincenzo, Phys. Rev. B, **59**, 2070 (1999).
- [13] More traditionally, the linear combinations  $S(1,1) \equiv [ |L_{\uparrow}R_{\downarrow}\rangle - |L_{\downarrow}R_{\uparrow}\rangle ]/\sqrt{2}$  and  $T_0(1,1) \equiv [ |L_{\uparrow}R_{\downarrow}\rangle + |L_{\downarrow}R_{\uparrow}\rangle ]/\sqrt{2}$ , are employed.
- [14] J. M. Taylor, *et al.*, Phys. Rev. B **76**, 035315 (2007).
- [15] Coulomb matrix elements are defined in the usual way in our two state basis,  $\alpha, \beta, \gamma, \delta \in \{L, R\}$ :  $V_{\alpha\beta\gamma\delta} \equiv \int \int d\mathbf{r}_1 d\mathbf{r}_2 \psi_{\alpha}^*(\mathbf{r}_1) \psi_{\beta}^*(\mathbf{r}_2) V(\mathbf{r}_1, \mathbf{r}_2) \psi_{\gamma}(\mathbf{r}_1) \psi_{\delta}(\mathbf{r}_2)$ .
- [16] We have also used the identity:  $\mathbf{S} \cdot \mathbf{I}_m = S_z I_{mz} + [S_- I_{m+} + S_+ I_{m-}]/2$ .
- [17] M. Stopa, unpublished.
- [18] J. R. Petta *et al.*, Science **309**, 2180 (2005).
- [19] D. Paget *et al.*, Phys. Rev. B **15**, 5780 (1977).
- [20] Self consistent electronic structure calculations show (Stopa, unpublished) that for lateral double quantum dots,  $V_x$  can range from  $250 \mu V$  to less than  $1 \mu V$ . Here, we have chosen the lower value.
- [21] M. Gullans *et al.*, in preparation.
- [22] W. Yao arXiv:0905.2460v1